SECOND EUROPEAN CONFERENCE ON EARTHQUAKE ENGINEERING
AND SEISMOLOGY, ISTANBUL AUG. 25-29, 2014

CO-SEISMIC PERMANENT GROUND DISPLACEMENTS IN SOUTH ICELAND

Rajesh RUPAKHETY[1] and Ragnar SIGBJÖRNSSON[2]

ABSTRACT

This contribution presents and discusses permanent ground displacements in the near-fault area of three recent earthquakes in the South Iceland Seismic Zone. Permanent ground displacements are obtained by processing ground acceleration time series according to an algorithm developed by Rupakhety et al. (2010). The ground acceleration time series are the ones recorded during the 17 June 2000 Mw 6.5 Earthquake, the 21 June 2000 Mw 6.5 Earthquake, and the 29 May 2008 Mw 6.3 Ölfus Earthquake. Data at 25 stations with epicentral distance in the range of 3km to 22km are considered. Significant permanent ground displacements, about half a meter at some of the stations closest to the fault, are observed. The observed displacements seem to attenuate apparently linearly with distance from the source. The spatial distribution of permanent displacement in the near-fault area is consistent with their estimates based on GPS data. Furthermore, the sense of permanent displacements around the faults clearly depict right-lateral faulting mechanism characteristic of earthquakes in the study area. Particle displacement at stations located on opposite sides of fault is found to be remarkably symmetric.

INTRODUCTION

During strong shallow crustal earthquakes, ground surface in the vicinity of the earthquake source is often permanently displaced. Although transient ground displacement waves travel great distance from the source, the permanent pseudo-static displacements can be observed only in a relatively small area around the source. Estimates of permanent ground displacements can serve both seismological and engineering community. Co-seismic displacements are useful to infer slip on the fault plane and thereby impose reliable constraints on physical models of rupture. In earthquake resistant design, an estimate of expected permanent displacement is particularly useful for designing infrastructure and lifeline systems. For example, damage to buried pipelines and lifeline systems crossing active geological faults is governed by earthquake-induced permanent ground displacements (see, for example, Priestley and Calvi, 2002). When GPS measurements are available, permanent ground displacements can be estimated relatively confidently. However, such measurements are scarce, and for a long time, engineering seismologists have attempted to recover approximate displacement estimates from ground acceleration time series obtained from strong motion records.

In theory, ground velocity and displacement can be accurately computed if 6-component (3 translational and 3 rotational) acceleration data are available (Graizer, 1989). Unfortunately, most strong motion instruments record only 3 translational components of ground acceleration. With high-quality digital data, it is, in some cases, possible to extract long-period motion—including permanent displacements—from the 3-component translational accelerometric data. Integrating ground acceler-

[1] Associate Professor, Earthquake Engineering Research Center, 800 Selfoss, Iceland, rajesh@hi.is
[2] Professor, Earthquake Engineering Research Center, 800 Selfoss, Iceland, ragnar.sigbjornsson@hi.is

ation data, however, is not a straightforward task, as it is often contaminated by various artificial and extraneous additions, collectively called noise, the integration of which is a very unstable operation. Different algorithms have been developed by researchers to supress the effects of noise so that estimates of ground velocity and displacement may be obtained by successive integration of ground acceleration (see, Rupakhety et al., 2010, for a detailed review).

This contribution applies the baseline adjustment technique developed by Rupakhety et al. (2010). The application of this method to ground acceleration data recorded in various earthquakes around the world has yielded permanent displacement estimates that are in good agreement with GPS measurements (see, for example, Rupakhety et al., 2010; Rupakhety and Sigbjörnsson, 2010). In this contribution, we utilize this method to estimate permanent ground displacements in the near-fault area of recently recorded earthquakes in South Iceland Seismic Zone (SISZ). Following a description of the ground-motion data, some samples of computed displacement time histories are presented. The spatial distribution of permanent displacements in the near-fault are then mapped and discussed.

STRONG-MOTION DATA

The strong-motion data applied in this study are obtained from three recent earthquakes in South Iceland Seismic Zone. The three earthquakes are the 17 June 2000 Mw 6.5 South Iceland Earthquake, the 21 June 2000 Mw 6.4 South Iceland Earthquake, and the 29 May 2008 Mw 6.3 Ölfus Earthquake. More details about the earthquakes and their effects can be found in Sigbjörnsson et al. (2007, and 2009). These earthquakes were recorded by the Icelandic Strong Motion Network (Sigbjörnsson, 1990). The recorded ground acceleration data are available on the ISESD (Internet Site for European Strong-Motion Data) online database (Ambraseys et al., 2004). The Ölfus earthquake was also recorded by a dense strong-motion array (ICEARRAY) located in a village near the earthquake fault (see, Halldorsson and Sigbjörnsson, 2009). Permanent ground displacements obtained from the ICEARRAY recordings have been presented in Rupakhety et al. (2010). This study focuses on ground displacements obtained from accelerometric records of the June 2000 earthquakes. The details of the recording stations are shown in Table 1. Accelerometric records from six stations (1-6) from the 17 June 2000 earthquake and seven stations (2, 4, 5-9) are used in this study.

Table 1. Recording stations with permanent ground displacement during the June 2000 earthquakes

Number	Station	Location	
		Latidude (° N)	Longitude (° W)
1	Flagbarnarholt	63.991	20.064
2	Kaldarholt	64.004	20.474
3	Minni–Nupur	64.050	20.160
4	Hella	63.840	20.390
5	Thjorsarbru	63.931	20.649
6	Solheimar	64.065	20.642
7	Thjorsartun	63.928	20.648
8	Selfoss Hospital	63.940	20.987
9	Selfoss Town Hall	63.937	21.002

METHODOLOGY

The baseline adjustment scheme used in this work is described in detail in Rupakhety et al. (2010). The method is primarily based on the works of Iwan et al. (1985) and Wu and Wu (2007). The baseline shift model is the same as that of Iwan et al. (1985). Assuming that the ground displacement resembles a ramp function, we use the corresponding Fourier amplitude spectra of ground velocity to calibrate the baseline shift. This is achieved by maximizing the flatness of ground velocity Fourier amplitude spectra at the low frequency side of the spectrum. This model yields stable estimates of permanent ground displacements which have been shown in Rupakhety et al. (2010) to be similar to the estimates obtained from GPS measurements. The long-period noise caused by baseline offsets and possibly instrument tilt is effectively reduced, resulting in a ground velocity time series that reduces to

zero and a ground displacement time series that reaches a stable value at the end. The effectiveness of the proposed method is demonstrated with an example shown in Fig.1. Similar results were obtained at other stations recording the two earthquakes of June 2000. These results are summarized in the next Section.

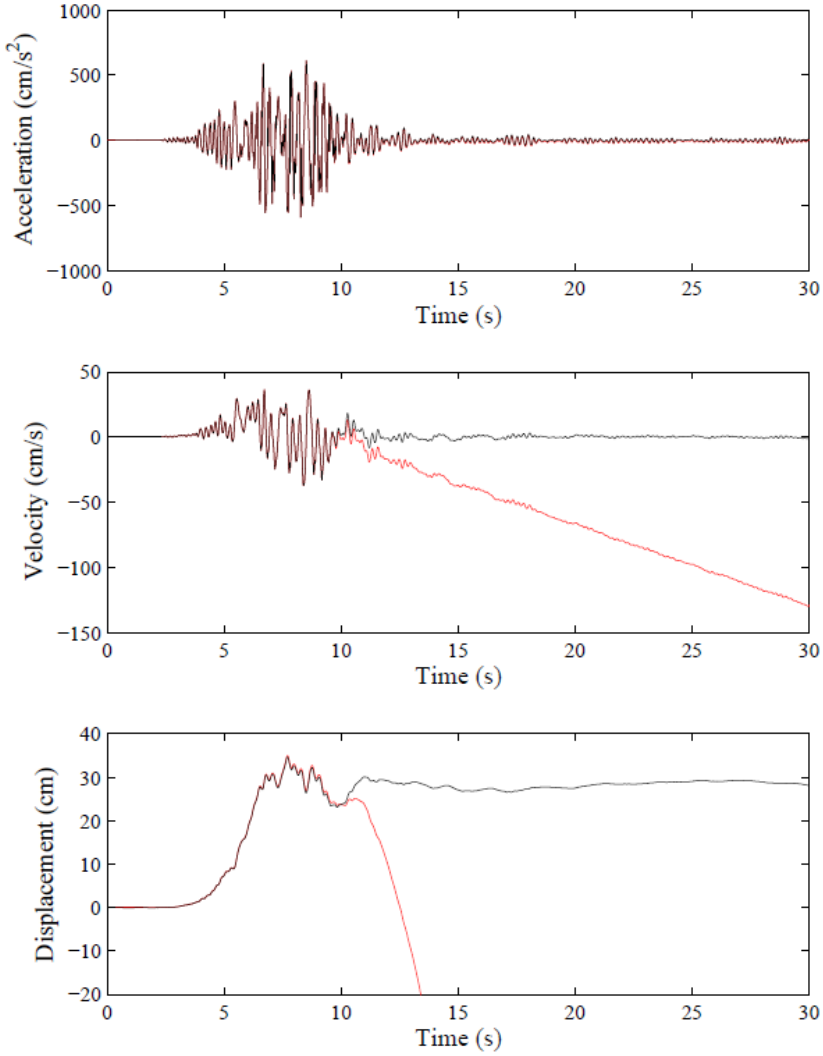

Figure 1. Recorded acceleration (top), derived velocity (middle), and derived displacement (bottom) time histories of N-S ground motion at Kardarholt station during the 17 June 2000 South Iceland Earthquake. The station is located about 4 km from the causative fault. Raw (mean removed) acceleration and the corresponding velocity and displacement obtained by successive integration are shown in red. The corresponding ground-motion time series obtained after applying baseline adjustment are shown in black. Note that the baseline adjustment has negligible effect on ground acceleration, but significantly improves ground velocity and displacement time series. Linear drift observed in raw velocity and quadratic drift observed in raw displacement are effectively removed to obtain stable and physically meaningful ground velocity and displacement time series.

RESULTS

This section provides a summary of permanent ground displacements recovered from ground acceleration recorded at different stations during the June 2000 earthquakes. A visualisation of the recovered displacements is provided along with maps showing their spatial distribution and comparison with the permanent displacements obtained from GPS measurements. An example of particle motion at two stations across the fault is also presented.

Permanent displacements

Permanent ground displacements recovered from ground acceleration recorded at different stations are summarized in Table 2. For each station the station identification number of the ICESMN is shown in the table. The raw ground acceleration data can be obtained from the ISESD by referring to the Waveform Identification (WID) as shown in the table. The Joyner-Boore distance of the recording station from the earthquake sources are taken from Halldorsson et al. (2007). Permanent ground displacements in the North-South (N-S) and the East-West (E-W) directions are shown in the last two columns of the table. Considerable permanent displacements, almost half a meter, are observed at stations located close to the fault. Some permanent displacements are obtained at stations as far as around 14 km from the earthquake faults.

Table 1. Permanent ground displacements recovered from ground acceleration records

Earthquake Date	Station	SID*	WID**	Joyner-Boore distance r_{JB} (km)	Permanent displacement (cm)	
					N-S	E-W
17 June 2000	Flagbjarnarholt	106	4674	4.2	-23	19
	Kaldarholt	103	6263	5.4	28	-25
	Minni-Nupur	108	4675	9.0	-15	-1
	Hella	105	4673	6.5	17	-3
	Thjorsarbru	502	6277	13.3	-8	-6
	Solheimar	109	4676	14.1	5	-9
21 June 2000	Thjorsarbru	502	6349	2.8	-16	47
	Thjorsartun	107	6332	2.9	-7	48
	Solheimar	109	6334	4.1	-25	-23
	Kaldarholt	103	6328	11.0	-6	13
	Selfoss Hospital	101	6326	13.0	7	7
	Selfoss Town Hall	112	6335	13.7	4	4
	Hella	105	6330	17.1	4	4

* Station identification number of the ICESMN

** Waveform identification number of the selected record in ISESD (Ambraseys et al., 2004)

Permanent horizontal ground displacements in the near-fault area of the 17 June event are shown with red arrows in Fig. 2. Largest displacements are observed at stations 103 and 106, which are also the two closest stations to the fault. The resultant horizontal displacements at these stations were computed to be 38 cm and 30 cm, respectively. These two stations are almost equidistant from the Holt fault and are located on its opposite sides. The sense of ground displacement at these two stations clearly reflects the right lateral strike slip faulting mechanism of the earthquake. The stations 106 and 103 moved relative to each other by 51 cm in the fault parallel direction. These estimates can be useful in constraining models of co-seismic slip on the fault plane. Slip on the fault plane based on uniform and distributed models for the 17 June event have been estimated in several studies (see, for example, Dubios et al., 2008, and references therein). The slip model of Dubios et al. (2008) predicts a slip of ~1.5 m at a point on the fault closest to station 103. Considering attenuation of co-seismic displacement with distance from the fault, the related motion across stations 103 and 106 obtained in this study seem to be in good agreement with the slip model of Dubios et al. (2008) which was inferred from GPS and InSAR data. Stations 502 and 107 (see Fig.1) are located very close to each other. Station 502 is located on a bridge pier on the west bank of Thjorsa River. Station 107 is located on a farm named Thjorsartun on top of a small hill, on the eastern bank of the river. The western bank of the river is formed on lava rock overlaying soft sediments, where evidence of soil amplification at frequencies above 2.5 Hz has been reported (Bessason and Kaynia, 2002). As permanent displacements are governed by much smaller frequencies than the fundamental frequency of soil, soil effects in their estimates are not expected to be significant, which is confirmed by our results from the 21 June 2000 Earthquake (see Table 2). A similar comparison could not be made for the 17 June event as station 107 did not record that event.

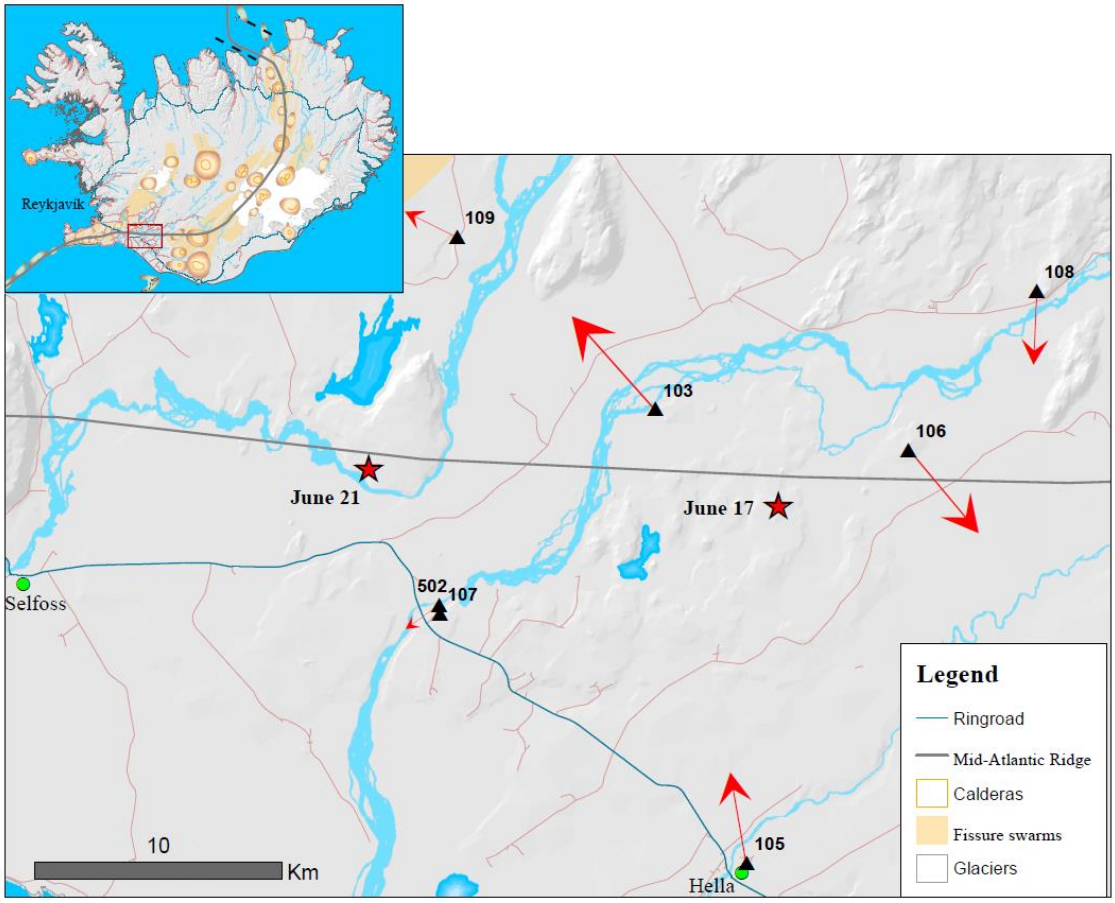

Figure 2. Permanent ground displacements in the near fault area of the 17 June 2000 South Iceland Earthquake. The inset on top left corner shows a map of Iceland with main geological formations as described in the legend. The area indicated by the red rectangle on the inset map is shown in the main figure. Triangles on the map indicate the locations of accelerometers that recorded the 17 June earthquake. The epicentres of the two earthquakes are marked with red starts. The faulting mechanism is of the right lateral strike-slip type. The red arrows originating at the stations indicate the magnitude, direction and sense of permanent ground displacement. The plotted displacements are those contributed by the 17 June event alone. Permanent ground displacements in the N-S and E-W directions are provided in Table 2.

Comparison with GPS measurement

In order to check the validity of the estimated permanent ground displacements, it is useful to compare the results with estimates from other independent studies. If there were continuous measurement at GPS stations collocated with the strong-motion stations, GPS data could be used as a reference for verifying and validating the results obtained from strong-motion data. Unfortunately, there are not any collocated or nearby continuous GPS stations in the study area. However, GPS surveys were conducted in the area in 1986, 1989, 1992, 1995, 1999, and 2000. Arnadottir et al. (2001) used GPS measurements from the 1995, 1999, and 2000 surveys to estimate co-seismic displacements caused by the June 2000 earthquakes. Because GPS survey data between the 17 June and 21 June events are not available, the contribution of the two events to the total permanent ground displacements could not be separated. To compare the results of GPS data (Arnadottir et al., 2001), permanent ground displacements estimated from strong-motion data (see Table 2) from the two events were summed to estimate total displacements.

In Fig 3, the total horizontal displacement vectors obtained from recorded ground acceleration are plotted as red arrows. Those obtained from GPS measurements are plotted as blue arrows. It should be noted that station 107 did not record the 17 June event, and therefore the total displacement

at this station shows the contribution of only the 21 June event. The pattern of GPS results shown in Fig. 3 is similar to the results obtained from recorded ground acceleration. Permanent displacement computed at Thjorsarbru Bridge, denoted as 502 in Fig. 3, is in very close agreement with the results obtained from GPS measurement at a nearby station. The displacement computed at Thjorsartun, marked as 107 in Fig. 3, shows some deviation from the one computed at station 502. However, from Table 2, it is clear that the displacements computed at stations 502 and 107 due to the 21 June event are almost the same. The apparent difference in total displacement is due to the fact that station 107 did not record the 17 June event.

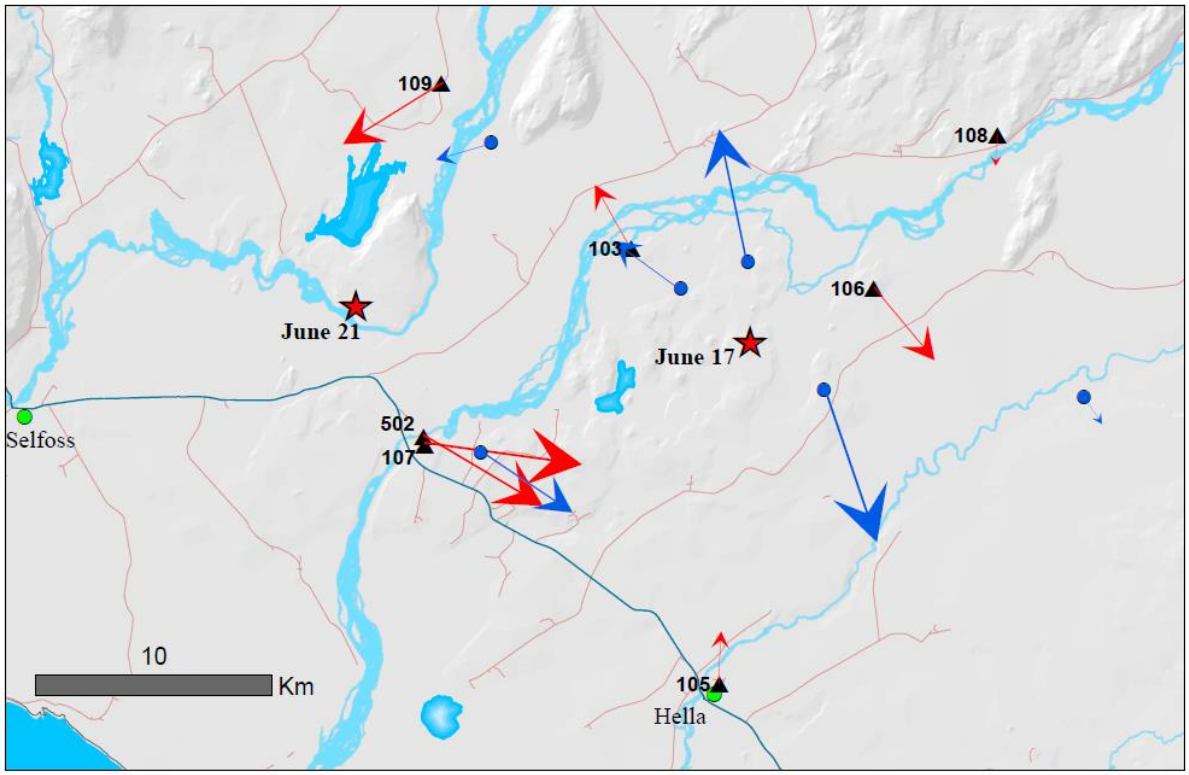

Figure 3. Permanent ground displacements in the near fault area of June 2000 earthquakes. The effects of both the 17 June and the 22 June events are summed to plot the horizontal permanent ground displacements as shown with red arrows. The blue arrows represent permanent ground displacements obtained from GPS measurements (Arnadottir et al., 2001).

Particle motion across the fault

Displacement time histories at stations close to the fault can provide information on the evolution of displacement on the fault. Careful study of displacement time histories at stations lying on the opposite sides of the fault may indicate important physical phenomena, for example, the faulting mechanism. An example of such study is presented here. The study is based on ground displacement at Flagbjarnarholt and Kaldarholt during the 17 June 2000 Earthquake. These stations are marked as 106 and 103 in Fig. 3. Both of these stations are within 5 km distance from the fault. Flagbjarnarholt lies to the east and Kaldarholt lies to the east of the Holt fault, where the 17 June 2000 Earthquake occurred.

In Fig. 4, particle displacements at these stations are projected on the horizontal plane. The black and green traces represent motion at Flagbjarnarholt and Kaldarholt, respectively. Fault-parallel and fault-normal displacements are plotted in the vertical and the horizontal axes, respectively. The displacement time histories at these stations are remarkably symmetric. The relative motion across the two stations clearly indicates a right-lateral mechanism. Initially, Flagbjarnarholt moves south-west and Kaldarholt moves north-east. Then the fault-normal motion changes, with Flagbjarnarholt moving towards east and Kaldarholt towards west. This sense of south-east north-west motion remains steady for a major part of ground shaking. Towards the end of shaking, the two stations slightly bounce back

towards each other. Finally, Kaldarholt is permanently displayed to the north-west of its initial position and Flabjarnarholt is permanently displaced to the south-east of its initial position. Similar observations can be made from the particle motion projected on a vertical plane parallel to the fault strike shown in Fig. 5. The symmetry of the particle motion is remarkable, but expected due to the symmetrical positioning of these two stations across the fault plane. Such symmetry and simplicity in the motion pattern is not evident in ground acceleration at these stations, most likely due to the dominance of high-frequency oscillations.

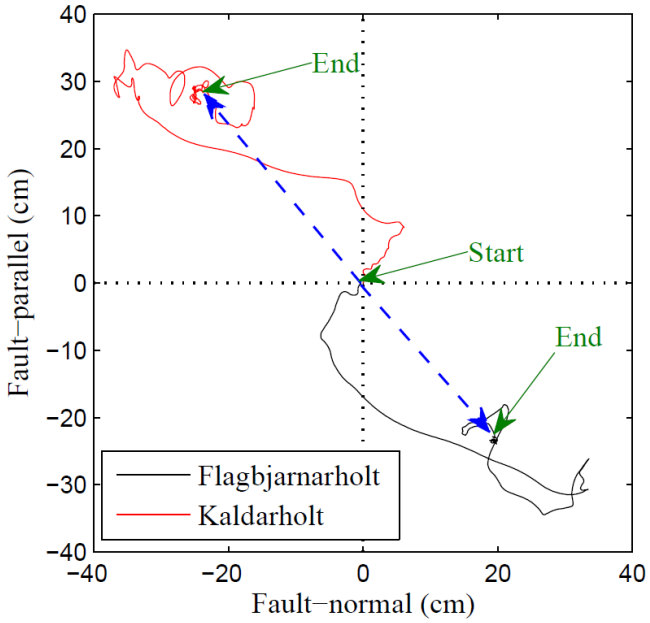

Figure 4. Projection of particle displacement on the fault-normal and the fault-parallel directions. North and East are plotted as positive. The blue arrows indicate the final displacement.

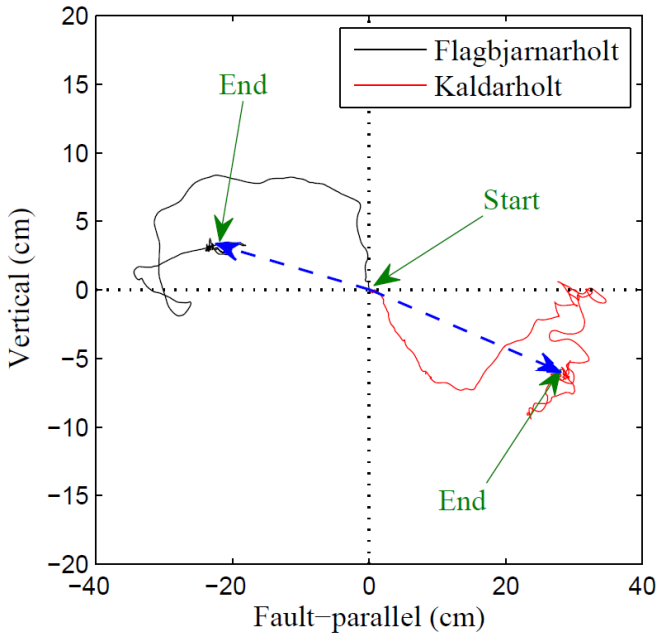

Figure 4. Projection of particle displacement on a vertical plane parallel to the fault strike. Upwards and northwards displacements are plotted as positive. The blue arrows indicate the final displacement.

Attenuation of permanent ground displacement

Permanent ground displacements are observed in a limited area close to the fault. This implies that the pseudo-static effect resulting in permanent ground displacement attenuates fast from the fault. Although the data available in the study region is not sufficient to calibrate a well-constrained attenuation equation for permanent ground displacement, some insight into it can be gained by studying its dependence on the distance from the fault plane. To study this dependence, we use permanent ground displacements from the 17 June 2000 South Iceland Earthquake, 21 June 2000 South Iceland Earthquake, and 29 May 2008 Ölfus Earthquake. The computed displacements obtained from the 29 May 2008 Ölfus Earthquake are as reported in Rupakhety et al. (2010). Epicentral distance is considered to represent source to site distance. Other distance metrics, such as Joyner-Boore distance, might be more appropriate in this regard. However, the Ölfus Earthquake ruptured two nearby faults simultaneously, and therefore, distance metrics based on a single rupture surface are not sufficient. Epicentral distance of the stations recording the Ölfus earthquake is based on a macroseismic epicentre and are as reported in Rupakhety and Sigbjörnsson (2009).

The variation of permanent ground displacement with epicentral distance is shown in Fig. 5 for the three recent earthquakes in South Iceland. Observations from the three earthquakes are marked with different symbols as indicated in the figure legend. Close to the fault, displacements almost equal to half a meter were observed during the 21 June Earthquake. With increasing source-site distance, permanent ground displacement attenuates fast and is expected to be negligible at a distance of around 30 km from the fault. We emphasize that this observation is valid only for moderate sized earthquakes like the ones studied here. For larger earthquakes, permanent ground displacements may be observed at larger distances from the source. The data available in the study area is not sufficient to draw reliable conclusions regarding the effect of earthquake magnitude. In general, it seems as expected, that permanent ground displacements increase with earthquake magnitude. However, there are a few exceptions with the 21 June Earthquake producing larger permanent displacements than the 17 June event. On the average, the dependence of permanent ground displacement with distance seems to be similar for the two June 2000 earthquakes. For the smaller event in May 2008, the attenuation seems to be faster than those of the June 2000 earthquakes.

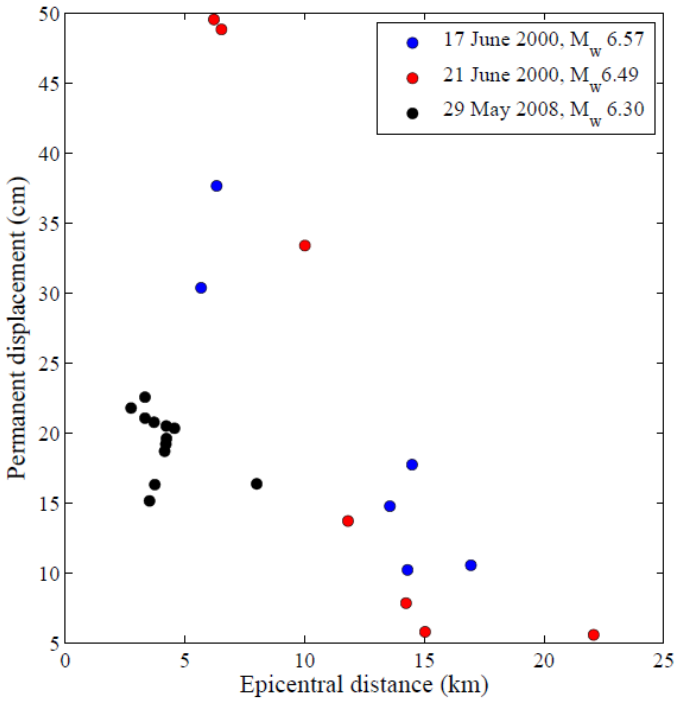

Figure 5. Permanent ground displacement as a function of epicentral distance for the three recent earthquakes in South Iceland (see explanation in the text).

CONCLUSIONS

Permanent ground displacements in the near-fault area of three large earthquakes in South Iceland—the 17 June 2000 Mw 6.5 Earthquake, the 21 June 2000 Mw 6.5 Earthquake, and the 29 May 2008 Mw 6.3 Ölfus Earthquake—are derived from ground acceleration data recorded during the earthquakes. The baseline adjustment algorithm used is proposed by Rupakhety et al. (2010), and this study, as well as other reported findings, reveals that it efficiently suppresses effects of long-period noise in the recorded data. The total number of stations where permanent ground displacement was observed is 25. The epicentral distance of these stations is in the range of 2.7 km to 22.1 km. At the closest stations to fault, permanent ground displacements nearly half a meter were observed during the 21 June 2000 Earthquake. The permanent ground displacement seems to attenuate rapidly with distance from the source, and is found to be negligible above 30 km distance for the range of magnitudes considered in this study. The general trend observed from the limited data is not enough to calibrate a well-constrained attenuation model, but some interesting patterns are observed. In general, permanent ground displacements seem to increase with earthquake size, with a few exceptions from the 21 June 2000 earthquake data. The rate of attenuation seems comparable for the two earthquakes in June 2000, but apparently lower for the Ölfus Earthquake. The reason for this discrepancy is not clear yet. Perhaps it is due to the fact that the Ölfus Earthquake ruptured two faults, parallel to each other, almost simultaneously. It is also worth mentioning that most of the data (except for one) obtained from the Ölfus earthquake lie on the same side (West) of the fault in the town of Hveragerði. One of the faults that ruptured during the earthquake is about 2 km east of Hveragerði and the other one is further 3 km to the east. The distance measures considered here are based on the macroseismic epicentre and therefore might not be representative of the source to site distance in terms of the distance from the rupture areas on the two faults. For example, the distance of Selfoss Town Hall to the western fault is smaller than its distance to the macroseismic epicentre. This is probably the reason why the displacement computed here seems to have attenuated slower than expected.

The permanent ground displacements obtained in this study are in good agreement with GPS and InSAR based measurements reported in the literature. The spatial distributions of permanent displacement around the fault plane clearly depict the right-lateral faulting mechanism of the three earthquakes. Particle motion at two stations located symmetrically to the fault of the 17 June event displayed some interesting features. The ground displacements at these stations were found to be remarkably symmetric. With development of dense strong-motion networks in seismically active areas around the world, estimates of permanent ground displacement in the near-fault stations will prove valuable in providing additional constraints on inferring slip distribution on the fault plane. It is our belief at study of particle displacement at near-fault stations might provide valuable insight into the mechanics of rupture propagation on the fault plane. The data available today is not sufficient to propose a quantitative approach to such applications. However, it is hoped that with more data recorded in the future, formulation of such applications will be realized.

REFERENCES

Ambraseys N, Smit P, Douglas J, Margaris B, Sigbjörnsson R, Ólafsson S, Suhadolc P, Costa G (2004) Internet site for European strong-motion data. *Bollettino di Geofisica Teorica ed Applicata* 45(3):113–129

Arnadottir Th, Hreinsdottir S, Gudmundsson G, Einarsson P, Heinert M, Volksen C (2001) Crustal deformation measured by GPS in the South Iceland Seismic Zone due to two large earthquakes in June 2000. *Geophysical Research Letters* 28(21):4031—4033

Bessason B, Kaynia AM (2002) Site amplification in lava rock on soft sediments. *Soil Dynamics and Earthquake Engineering* 22:525—540

Dubois L, Feigl KL, Komatitsch D, Arnadottir Th, Sigmundsson F (2008) Three-dimensional mechanical models for the June 2000 earthquake sequence in the south Iceland seismic zone. *Tectonophysics* 457:12—29

Graizer VM (1989) On inertial seismometry. *Izv Earth Phys* 25:26–29

Halldorsson B, Sigbjörnsson R (2009) The Mw 6.3 Ölfus earthquake at 15:45 UTC on 29 May 2008 in South Iceland: ICEARRAY strong-motion recordings. *Soil Dynamics and Earthquake Engineering* 29: 1073–1083

Halldorsson B, Olafsson S, Sigbjörnsson R (2007) A fast and efficient simulation of the far-fault and near-fault earthquake ground motions associated with the June 17 and 21, 2000, Earthquakes in South Iceland. *Journal of Earthquake Engineering* 11:343—370

Iwan WD, Moser MA, Peng CY (1985) Some observations on strong-motion earthquake measurement using a digital accelerograph. *Bulletin of Seismological Society of America* 75:1225–1246

Priestley MJN, Calvi GM (2002) Strategies for repair and seismic upgrading of Bolu Viaduct 1, Turkey. *Journal of Earthquake Engineering* 6(1):157–184

Rupakhety R, Halldórsson B, Sigbjörnsson R (2010) Estimating coseismic deformations from near source strong motion records: methods and case studies. *Bulletin of Earthquake Engineering* 8(4):787–811

Rupakhety R, Sigbjörnsson R (2009) Ground-Motion Prediction Equations (GMPEs) for inelastic response and and structural behaviour factors. *Bulletin of Earthquake Engineering* 7(3):637—659

Rupakehty R, Sigbjörnsson R (2010) A note on the L'Aquila earthquake of 6 April 2009: Permanent ground displacements obtained from strong-motion accelerograms. *Soil Dynamics and Earthquake engineering* 30(4):215—220

Sigbjörnsson R, Ólafsson S, Snæbjörnsson JTh (2007) Macroseismic effects related to strong ground motion: a study of the South Iceland earthquakes in June 2000. *Bulletin of Earthquake Engineering* 5(4):591–608

Sigbjörnsson R, Snæbjörnsson JTh, Higgins SM, Haldorsson B, Olafsson S (2009) A note on the M_w 6.3 earthquake in Iceland on 29 May 2008 at 15:45 UTC. *Bulletin of Earthquake Engineering* 7:113—126

Sigbjörnsson, R. (1990) Strong Motion Measurements in Iceland and Seismics Risk Assessment, *Proceedings of the 9th Conference on Earthquake Engineering*, The Kucherenko Tsniisk of the USSR Gosstroy, Moscow

WuY-M,Wu C-F (2007) Approximate recovery of coseismic deformation from Taiwan strong-motion records. *Journal of Seismology* 11:159–170